

Dynamical heavy-quark recombination and the nonphotonic single-electron puzzle at energies available at the BNL Relativistic Heavy Ion Collider (RHIC)

 Alejandro Ayala,^{1,2} J. Magnin,² Luis Manuel Montaño,³ and G. Toledo Sánchez⁴
¹*Instituto de Ciencias Nucleares, Universidad Nacional Autónoma de México, Apartado Postal 70-543, México Distrito Federal 04510, México*
²*Centro Brasileiro de Pesquisas Físicas, CBPF, Rua Dr. Xavier Sigaud 150, 22290-180 Rio de Janeiro, Brazil*
³*Centro de Investigación y de Estudios Avanzados del IPN, Apartado Postal 14-740, México Distrito Federal 07000, México*
⁴*Instituto de Física, Universidad Nacional Autónoma de México, Apartado Postal 20-364, México Distrito Federal 01000, México*
 (Received 21 September 2009; published 7 December 2009)

We show that the single, nonphotonic electron nuclear modification factor R_{AA}^e is affected by the thermal enhancement of the heavy-baryon-to-heavy-meson ratio in relativistic heavy-ion collisions with respect to proton-proton collisions. We make use of the dynamical quark recombination model to compute such a ratio and show that this produces a sizable suppression factor for R_{AA}^e at intermediate transverse momenta. We argue that this suppression factor needs to be considered, in addition to the energy loss contribution, in calculations of R_{AA}^e .

 DOI: [10.1103/PhysRevC.80.064905](https://doi.org/10.1103/PhysRevC.80.064905)

PACS number(s): 13.85.Qk, 25.75.Nq, 25.75.Ld

I. INTRODUCTION

The suppression of single, nonphotonic electrons at the BNL Relativistic Heavy Ion Collider (RHIC) [1,2] is usually attributed to heavy-quark energy losses. However, calculations that successfully describe the nuclear modification factor of hadrons fail to describe the single, nonphotonic electron nuclear modification factor R_{AA}^e [3–5]. This has prompted a great deal of effort aimed to better describe the heavy-quark energy-loss mechanisms to include not only the radiative part [6–9] but also the collisional [10,11] and the medium dynamical properties [12] to compute the radiative piece. As a result, although some improvement in the description of the nuclear modification factor has been gained, it is not yet clear whether the anomalous suppression can be completely attributed to energy losses.

Working along a complementary approach to describe the nonphotonic electron yield at RHIC, it has been argued [13,14] that under the assumption of an enhancement in the heavy-quark baryon-to-meson ratio, analogous to the case of the proton-to-pion and the Λ -to-kaon ratios in Au + Au collisions [15–18], it is possible to achieve a larger suppression of the nuclear modification factor. The rationale behind the idea is that heavy-quark mesons have a larger branching ratio to decay inclusively into electrons as compared with heavy-quark baryons, and therefore, when the former are less copiously produced in a heavy-ion environment, the nuclear modification factor decreases, even in the absence of heavy-quark energy losses in the plasma.

To give a qualitative argument that shows how an enhancement in the heavy-quark baryon-to-meson ratio can suppress the single, nonphotonic electron nuclear modification factor, let us look at the p_T integrated R_{AA}^e and consider that the heavy hadrons are only those containing a single charm,

$$R_{AA}^{e\ p_T\text{int}} = \frac{1}{\langle n_p \rangle} \frac{N_{AA}^\Lambda B^{\Lambda \rightarrow e} + N_{AA}^D B^{D \rightarrow e}}{N_{pp}^\Lambda B^{\Lambda \rightarrow e} + N_{pp}^D B^{D \rightarrow e}}, \quad (1)$$

where $\langle n_p \rangle$ is the average number of participants in the collision for a given centrality class, N_{AA}^x (N_{pp}^x) refers to the

number of x particles produced in $A + A(p + p)$ collisions, and $B^{x \rightarrow e}$ is the branching ratio for the inclusive decay of x particles into electrons. Let us bring Eq. (1) into a form that contains the corresponding p_T integrated nuclear modification factor for particles containing charm. We write

$$R_{AA}^{e\ p_T\text{int}} = \frac{1}{\langle n_p \rangle} \left(\frac{N_{AA}^D}{N_{pp}^D} \right) \left(\frac{B^{D \rightarrow e} + \frac{N_{AA}^\Lambda}{N_{pp}^\Lambda} B^{\Lambda \rightarrow e}}{B^{D \rightarrow e} + \frac{N_{pp}^\Lambda}{N_{pp}^D} B^{\Lambda \rightarrow e}} \right). \quad (2)$$

Let us introduce the shorthand notation

$$C = \frac{N_{AA}^\Lambda / N_{AA}^D}{N_{pp}^\Lambda / N_{pp}^D}, \quad (3)$$

$$x = \frac{B^{\Lambda \rightarrow e}}{B^{D \rightarrow e}},$$

where C represents the *enhancement factor* for the ratio of charm baryons to mesons in $A + A$ as compared with $p + p$ collisions and x is the charm baryon-to-meson relative branching ratios for their corresponding inclusive decays into electrons. With these definitions, and after rewriting the factor N_{AA}^D / N_{pp}^D in the form

$$\begin{aligned} \frac{N_{AA}^D}{N_{pp}^D} &= \frac{N_{AA}^D + N_{AA}^\Lambda - N_{AA}^\Lambda}{N_{pp}^D + N_{pp}^\Lambda - N_{pp}^\Lambda} \\ &= \left(\frac{N_{AA}^D + N_{AA}^\Lambda}{N_{pp}^D + N_{pp}^\Lambda} \right) \left[\frac{1 - N_{AA}^\Lambda / (N_{AA}^D + N_{AA}^\Lambda)}{1 - N_{pp}^\Lambda / (N_{pp}^D + N_{pp}^\Lambda)} \right], \end{aligned} \quad (4)$$

we can express Eq. (2) as

$$\begin{aligned} R_{AA}^{e\ p_T\text{int}} &= \frac{1}{\langle n_p \rangle} \left(\frac{N_{AA}^D + N_{AA}^\Lambda}{N_{pp}^D + N_{pp}^\Lambda} \right) \left[\frac{1 - N_{AA}^\Lambda / (N_{AA}^D + N_{AA}^\Lambda)}{1 - N_{pp}^\Lambda / (N_{pp}^D + N_{pp}^\Lambda)} \right] \\ &\quad \times \left(\frac{1 + Cx N_{pp}^\Lambda / N_{pp}^D}{1 + x N_{pp}^\Lambda / N_{pp}^D} \right) \\ &\equiv \frac{1}{\langle n_p \rangle} \left(\frac{N_{AA}^D + N_{AA}^\Lambda}{N_{pp}^D + N_{pp}^\Lambda} \right) T_{AA}^{e\ p_T\text{int}}. \end{aligned} \quad (5)$$

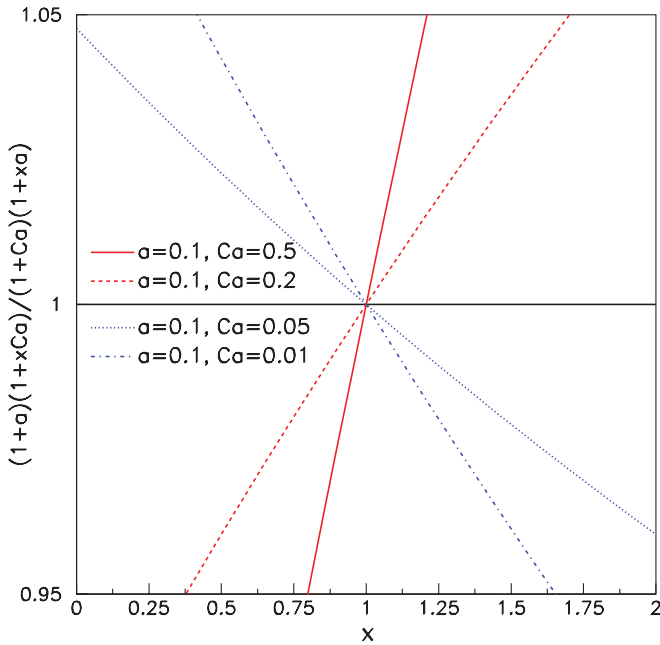


FIG. 1. (Color online) p_T integrated T_{AA}^e as a function of x , the ratio of branching ratios for charmed baryons and mesons to decay inclusively into electrons. Notice that for $x < 1$, $T_{AA}^e < 1$ when Ca (the ratio of charm baryons to mesons in $A + A$) is larger than a (the ratio of charm baryons to mesons in $p + p$).

When not integrated over transverse momentum, the factor $1/\langle n_p \rangle [(N_{AA}^D + N_{AA}^\Lambda)/(N_{pp}^D + N_{pp}^\Lambda)]$ represents the nuclear modification factor for particles with charm. Let us not assume any particular value for this factor and instead concentrate on the other one in Eq. (5), which can be written as

$$T_{AA}^{e \text{ print}} = \frac{(1+a)(1+xCa)}{(1+Ca)(1+xa)}, \quad (6)$$

where $a = N_{pp}^\Lambda/N_{pp}^D$. The quantity in Eq. (6) is plotted in Fig. 1 as a function of x for different combinations of Ca and a . Notice that the function $T_{AA}^{e \text{ print}}$ is less than 1 when $x < 1$ provided that $Ca > a$.

In this work, we want to quantitatively address the question of whether the enhancement factor C times a —namely, the heavy-baryon-to-heavy-meson ratio in $Au + Au$ collisions—can indeed be larger than a —namely, the heavy-baryon-to-heavy-meson ratio in $p + p$ collisions—and if so, how this affects the behavior of the factor T_{AA}^e as a function of p_T . For these purposes, we use a dynamical recombination scenario that accounts for the fact that the probability to form baryons and mesons can depend in a different way on the evolving density during the collision. A coalescence model addressing the same goals has been recently presented in Ref. [19].

The work is organized as follows: After presenting a brief introduction to the dynamical quark recombination model in Sec. II, we proceed in Sec. III to compute the probabilities to form mesons and baryons containing a heavy quark in a relativistic heavy-ion collision environment. In Sec. IV, we use these probabilities to write expressions for the meson

and baryon transverse-momentum distributions. In Sec. V, we compute such distributions as well as the baryon-to-meson ratio. We convolute this ratio with the branching ratios of charmed baryons and mesons to decay into electrons to obtain the p_T unintegrated function T_{AA}^e and show that this can be indeed less than 1. Finally we summarize and conclude in Sec. VI.

II. DYNAMICAL QUARK RECOMBINATION

In its simplest form, the recombination of quarks explains the formation of low-to-intermediate p_T hadrons from the bounding of quarks in a densely populated phase space, assuming the appropriate degeneracy factors for mesons and baryons [20]. This scenario accounts only for correlations among quarks in momentum space and not for the expected correlations in coordinate space. Moreover, an implicit assumption is that hadronization happens at a single temperature.

However, hadronization is not an instantaneous process. In fact, lattice calculations [21] show that the phase transition from a deconfined state of quarks and gluons to a hadron gas is, as a function of temperature, not sharp. Working along this line of thought, it has recently been shown [22] that the features of the proton-to-pion ratio can be well described by means of the so-called *dynamical quark recombination model* (DQRM) that incorporates how the probability to recombine quarks into mesons and baryons depends on density and temperature. Other approaches toward a dynamical description of recombination have been recently formulated [23].

The upshot of the DQRM is that the density evolving probability differs for hadrons made up by two and three constituents *with the same mass*; that is to say, the relative population of baryons and mesons can be attributed not only to flow but also to the dynamical properties of quark clustering in a varying density scenario. A natural question is whether those features remain true for baryons and mesons with one constituent heavy quark and whether a computed, as opposed to an assumed, baryon-to-meson ratio can at least partially explain the anomalous single, nonphotonic electron suppression at RHIC.

Recall that, on the one hand, for the kinematic regime where quark recombination happens, the assumption is that the recombining light flavors are thermal. On the other hand, the thermalization of heavy flavors has been a subject of intense research over the past years [24,25]. Nevertheless, it is not clear whether heavy flavors need to be thermal to recombine or else whether recombination can happen in a sort of *pickup* reaction where a heavy flavor, not necessarily thermal, coalesces with light quarks on its way out to form either mesons or baryons. In this work we employ the point of view that the recombination of heavy quarks happens without the need for these to be initially thermal, although the light quarks that the heavy quark coalesces with have already thermalized, producing a finally thermal hadron.

The invariant transverse-momentum distribution of a given hadron can be written as an integral over the freeze-out space-time hypersurface Σ of the relativistically invariant

phase-space particle density $F(x, P)$,

$$E \frac{dN}{d^3P} = g \int_{\Sigma_f} d\Sigma \frac{P \cdot u(x)}{(2\pi)^3} F(x, P), \quad (7)$$

where P is the hadron's momentum, $u(x)$ is a future-oriented unit four-vector normal to Σ , and g is the degeneracy factor for the hadron that takes care of the spin degree of freedom. The function $F(x, P)$ contains the information on the probability that the given hadron is formed.

To allow for a dynamical recombination scenario in a thermal environment, let us assume that the phase-space particle density $F(x, P)$ can be factorized into the product of a term containing the thermal occupation number, including the effects of a possible flow velocity, and another term containing the system energy density ϵ driven probability $\mathcal{P}(\epsilon)$, for the coalescence of partons into a given hadron. We thus write

$$F(x, P) = e^{-P \cdot v(x)/T} \mathcal{P}(\epsilon), \quad (8)$$

where $v(x)$ is the flow velocity. As we will show, the probability $\mathcal{P}(\epsilon)$ incorporates in a simple manner the information that the coalescing partons need to be close in configuration space as well as to have a not-so-different velocity.

To compute the probability $\mathcal{P}(\epsilon)$, it has been shown in Ref. [22] (where we refer the reader to for details) that use can be made of the *string flip model* [26–28] to obtain information about the likelihood of clustering of constituent quarks to form hadrons from an effective quark-quark interaction. In short, the model is a variational quantum Monte Carlo simulation that, taking a set comprising an equal number of all color quarks and antiquarks at a given density, computes the optimal configuration of colorless clusters (baryons or mesons) by minimizing the potential energy of the system. At low densities, the model describes the system of quarks as isolated hadrons, whereas at high densities, this system becomes a free Fermi gas of quarks. The interaction between quarks is pairwise and taken as harmonic. The optimal clustering is achieved by finding the pairing producing the minimum in the potential energy between two given sets of quarks of different color for all possible color charges.

For *mesons*, the pairing potential V_{mes} is imposed to be between color and anticolor, allowing only the building up of pairs. For *baryons*, the pairing potential V_{bar} is imposed to be between the different colors in all possible combinations of colorless clusters, by linking 3, 6, . . . etc. quarks. Because the interaction is pairwise, the three-quark clusters are of the delta (triangular) shape.

To describe the evolution of a system of N quarks as a function of the particle density, we consider the quarks moving in a three-dimensional box, whose sides have length L , and the system described by a variational wave function of the form:

$$\Psi_\lambda(\mathbf{x}_1, \dots, \mathbf{x}_N) = e^{-\lambda V(\mathbf{x}_1, \dots, \mathbf{x}_N)} \Phi_{\text{FG}}(\mathbf{x}_1, \dots, \mathbf{x}_N), \quad (9)$$

where λ is the single variational parameter, $V(\mathbf{x}_1, \dots, \mathbf{x}_N)$ is the many-body potential for either mesons or baryons, and $\Phi_{\text{FG}}(\mathbf{x}_1, \dots, \mathbf{x}_N)$ is the Fermi gas wave function given by a product of Slater determinants, one for each color-flavor combination of quarks, which are built up of single-particle wave functions describing a free particle in a box [28]. The square of the variational wave function is the weighting probability

in the sampling, which we carry out using the metropolis algorithm. We can identify the value of the variational parameter λ as being directly proportional to the probability to form a cluster. This fact will be later exploited to define the density-dependent probability $\mathcal{P}(\epsilon)$ because, as we will show, λ changes from a fixed value at low density (isolated clusters) to zero at high density (Fermi gas).

III. PROBABILITIES

All the results we present here come from simulations done with 384 particles, 192 quarks and 192 antiquarks, corresponding to having 32 light quarks and 32 heavy quarks, plus their antiquarks in the three color charges (anticharges). Hereafter we refer to light quarks as u quarks and to the heavy ones as c quarks. The number of quarks corresponds to the second closed shell of a three-dimensional box. We have checked that for this number of particles, the errors associated with finite size are already negligible. The equal amounts of u and c quarks used in the simulation are not intended to represent the whole system but the relative fraction that drives the recombination. As we will explain, in the simulation, the relative abundance of baryons and mesons containing one c quark depends on the initial number of u and c quarks. We choose to work with equal numbers of each kind of quarks and at the end convert the relative fraction of resulting baryons and mesons to implement the physical conditions requiring that the number of c quarks be small compared with the number of u quarks [see Eq. (14)]. To take into account the mass difference between the u and c quarks, we set $m_c = 10m_u$. We have checked that variations of this particular choice do not affect our relative probabilities.

To determine the variational parameter as a function of density, we first select the value of the particle density ρ in the box, which for a fixed number of particles means adjusting the box size. Then, we compute the energy of the system as a function of the variational parameter using the Monte Carlo method described in the previous section. The minimum of the energy determines the optimal variational parameter. We repeat the procedure for a set of values of the particle densities in the region of interest. To get a measure of the probability to form a cluster, we take the variational parameter and divide it by its corresponding value at the lowest density. Notice that because the heavy quarks are not as abundant as the light ones, they do not contribute to the energy density, and thus, within the model, this last can be computed by assuming that only light flavors contribute.

The information contained in the variational parameter is global in the sense that it only gives an approximate idea about the average size of the interparticle distance at a given density, which is not necessarily the same for quarks in a single cluster. To correct for this, and to find an appropriate measure of the probability to form baryons and mesons, we need to multiply these variational parameters by the likelihood to find clusters of baryons made up of two-light, one-heavy quark and mesons made up of one-light, one-heavy quark. This likelihood has to consider the fact that the thermal plasma is mainly made up of light quarks and, thus, that the number of produced heavy

quarks is relatively small. To accomplish this, notice that in a model where the interaction between quarks to form clusters is flavor (as well as color) blind, this likelihood should account only for the combinatorial probabilities.

Consider the case where one starts out with a set of n , u quarks and m , c quarks, each coming in three colors. The number of possible colorless baryons containing three quarks of all possible flavors that can be formed are

$$\begin{array}{ll} \text{kind} & \text{number} \\ uuu & n^3 \\ uuc & 3n^2m \\ ucc & 3nm^2 \\ ccc & m^3, \end{array} \quad (10)$$

and the total number of possible baryons is $(n+m)^3$. The same counting applies for antibaryons when one starts from the same numbers of antiquarks instead of quarks.

Now, consider the case where one starts with a set of n , u quarks, n , \bar{u} antiquarks, m , c quarks, and m , \bar{c} antiquarks, each coming in three colors. The number of possible colorless mesons containing quark-antiquark pairs of all possible flavors that can be formed are

$$\begin{array}{ll} \text{kind} & \text{number} \\ u\bar{u} & 3n^2 \\ u\bar{c} & 3nm \\ \bar{u}c & 3nm \\ \bar{c}c & 3m^2, \end{array} \quad (11)$$

and the total number of possible mesons is $3(n+m)^2$. We now ask for the *relative* abundance of baryons with respect to mesons computed under the preceding assumptions on the number of light and heavy quarks that we start from. Because in the case of mesons we are considering the case $u\bar{c}$ as well as $\bar{u}c$, we need to include in the counting of the groups of three quarks also the antibaryons. Thus, the relative abundance is

$$\begin{aligned} \frac{c \text{ baryons} + c \text{ antibaryons}}{c \text{ mesons} + c \text{ antimsons}} &= \frac{2 \times 3n^2m/(n+m)^3}{2 \times nm/(n+m)^2} \\ &= \frac{3n}{2(n+m)}. \end{aligned} \quad (12)$$

Let us now impose that the number of u quarks be a multiple l of the number of c quarks, namely, $n = lm$. Therefore the preceding relative abundance can be written as

$$\frac{c \text{ baryons} + c \text{ antibaryons}}{c \text{ mesons} + c \text{ antimsons}} = \frac{3l}{2(l+1)}. \quad (13)$$

Notice that in the plasma, the number of u quarks greatly exceeds the number of c quarks. Therefore, a good analytical estimate of the preceding relative abundance can be obtained by taking $l \rightarrow \infty$, which gives

$$\frac{c \text{ baryons} + c \text{ antibaryons}}{c \text{ mesons} + c \text{ antimsons}} \xrightarrow{l \rightarrow \infty} \frac{3}{2}. \quad (14)$$

It can be checked that the asymptotic value $3/2$ is rapidly reached; for instance, by taking $l = 30$, the fraction in Eq. (14) already becomes 1.475.

Figure 2 shows the probability parameter $\mathcal{P}^{B,M}(\epsilon)$ for baryons and mesons, obtained by multiplying the variational

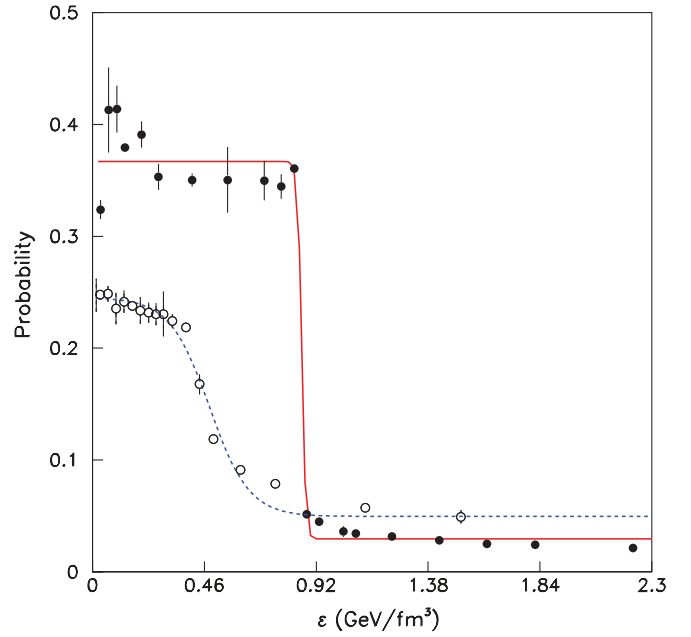


FIG. 2. (Color online) Probabilities $\mathcal{P}^{B,M}$ to produce charmed baryons and mesons as a function to the energy density ϵ . Shown are the results of the Monte Carlo simulation for baryons (full circles) and mesons (open circles) together with a fit to these.

parameter with the corresponding fraction of baryons/mesons formed at the given energy density. In the case of mesons, it corresponds to $1/4$ irrespective of the density, whereas for baryons, it has a functional form, because the kind of clusters can be different as density increases. For low densities, the ratio of the probabilities becomes $3/2$, as expected from the combinatorial described earlier. Also shown in the figure is a fit to the variational parameters with the functional form

$$f(x) = a_1 + \frac{a_2}{1 + \exp[(x - x_0)/dx]}. \quad (15)$$

For baryons

$$\begin{aligned} a_1^B &= 0.0294, \\ a_2^B &= 0.3374, \\ x_0^B &= 0.8604, \\ dx^B &= 0.0078, \end{aligned} \quad (16)$$

whereas for mesons

$$\begin{aligned} a_1^M &= 0.0496, \\ a_2^M &= 0.1953, \\ x_0^M &= 0.4812, \\ dx^M &= 0.0813. \end{aligned} \quad (17)$$

We will use this analytical expression to carry out the calculation of the spectra that we will proceed to describe.

IV. BARYON-TO-MESON RATIO

To quantify how the different probabilities to produce sets of three quarks as compared with sets of two quarks affect the particle's yields as the energy density changes during

hadronization, we need to resort to a model for the space-time evolution of the collision. We take Bjorken's scenario, which incorporates the fact that initially, expansion is longitudinal, that is, along the beam direction that we take as the \hat{z} axis, and include transverse flow as a small effect on top of the longitudinal expansion. In this scenario, the relation between the temperature T and the $1 + 1$ proper time τ is given by

$$T = T_0 \left(\frac{\tau_0}{\tau} \right)^{v_s^2}, \quad (18)$$

where $\tau = \sqrt{t^2 - z^2}$. Equation (18) assumes that the speed of sound v_s changes slowly with temperature. For simplicity, we take v_s as a constant equal to the ideal gas limit $v_s^2 = 1/3$.

We also consider that hadronization takes place on hypersurfaces Σ characterized by a constant value of τ , and therefore,

$$d\Sigma = \tau \rho \, d\rho \, d\phi \, d\eta, \quad (19)$$

where

$$\eta = \frac{1}{2} \ln \left(\frac{t+z}{t-z} \right), \quad (20)$$

is the spatial rapidity and ρ and ϕ are the polar transverse coordinates. Thus, the transverse spectrum for a hadron species H is given as the average over the hadronization interval of the right-hand side of Eq. (7), namely

$$E \frac{dN^H}{d^3P} = \frac{g}{\Delta\tau} \int_{\tau_0}^{\tau_f} d\tau \int_{\Sigma} d\Sigma \frac{P \cdot u(x)}{(2\pi)^3} F^H(x, P), \quad (21)$$

where $\Delta\tau = \tau_f - \tau_0$.

To find the relation between the energy density ϵ —that the probability \mathcal{P} depends on—and T , we resort to lattice simulations. For the case of two flavors (because the heavy quark does not thermalize), a fair representation of the data [21] is given by the analytic expression

$$\epsilon/T^4 = a \left[1 + \tanh \left(\frac{T - T_c}{bT_c} \right) \right], \quad (22)$$

with $a = 4.82$ and $b = 0.132$. We take $T_c = 175$ MeV.

The flow four-velocity vector v^μ is given by

$$v^\mu = (\cosh \eta \cosh \eta_T, \sinh \eta_T \cos \phi, \sinh \eta_T \sin \phi, \sinh \eta \cosh \eta_T), \quad (23)$$

where the magnitude of the transverse flow velocity v_T and η_T are related by $v_T = \tanh \eta_T$. The normal to the freeze-out hypersurfaces of constant τ , u^μ , is given by

$$u^\mu = (\cosh \eta, 0, 0, \sinh \eta). \quad (24)$$

We write the momentum four-vector in components as

$$P^\mu = (m_T \cosh y, p_T \cos \Phi, p_T \sin \Phi, m_T \sinh y), \quad (25)$$

where y is the $1 + 1$ momentum rapidity given by

$$y = \frac{1}{2} \ln \left(\frac{E + p_z}{E - p_z} \right) \quad (26)$$

and Φ is the azimuthal angle of the momentum components in the transverse plane.

Therefore, the products $P \cdot u$ and $P \cdot v$ appearing in Eq. (21) can be written as

$$\begin{aligned} P \cdot v &= m_T \cosh(\eta - y) \cos \eta_T - p_T \cos(\phi - \Phi) \sinh \eta_T, \\ P \cdot u &= m_T \cosh(\eta - y). \end{aligned} \quad (27)$$

Considering the situation of central collisions, we can assume that there is no dependence of the particle yield on the transverse polar coordinates. Integration over these variables gives

$$\begin{aligned} \frac{dN}{p_T dp_T dy} &= g \frac{m_T}{4\pi} \frac{\rho_{\text{nucl}}^2}{\Delta\tau} \int_{\tau_0}^{\tau_f} \tau d\tau \mathcal{P}(\tau) I_0(p_T \sinh \eta_T / T) \\ &\times \int d\eta \cosh(y - \eta) e^{-[m_T \cosh(y - \eta) \cosh \eta_T] / T}, \end{aligned} \quad (28)$$

where ρ_{nucl} is the radius of the colliding nuclei and I_0 is the Bessel function I of order zero.

We now consider as a further simplification that the space-time and momentum rapidities are completely correlated; that is, $\eta \sim y$. Under this assumption, the integral over η in Eq. (28) can be performed and we finally get

$$\begin{aligned} \frac{dN}{p_T dp_T dy} &= g \frac{m_T \Delta y}{4\pi} \frac{\rho_{\text{nucl}}^2}{\Delta\tau} \int_{\tau_0}^{\tau_f} \tau d\tau \mathcal{P}(\tau) \\ &\times I_0(p_T \sinh \eta_T / T) e^{-m_T \cosh \eta_T / T}. \end{aligned} \quad (29)$$

Armed with the expression to compute the hadron transverse-momentum distribution, we now proceed to apply the analysis to the computation of the charmed meson and baryon distributions.

V. RESULTS

Figure 3 shows examples of the transverse-momentum distributions for mesons and baryons obtained from Eq. (29). We set the masses of the charmed baryons and mesons as $m^B = 2.29$ GeV (corresponding to Λ_c) and $m^M = 1.87$ GeV (corresponding to D). We take the initial hadronization time as $\tau_0 = 1$ fm, at an initial temperature $T_0 = 200$ MeV, and the final hadronization temperature as $T_f = 100$ MeV, corresponding, according to Eq. (18), to a final time $\tau_f = 8$ fm. Shown are the cases with $v_T = 0$ and $v_T = 0.4$. Notice that a finite transverse expansion velocity produces a broadening of the distributions, as expected.

Figure 4 shows the charmed baryon-to-meson ratio obtained from the ratio of the preceding transverse-momentum distributions. Shown is a range for this ratio when varying the transverse expansion velocity v_T from 0 to 0.4. Notice that for a finite v_T , this ratio goes above 1 for $p_T \gtrsim 3.5$ GeV.

We now proceed to compute the p_T unintegrated function T_{AA}^e . For this purpose, we take that the possible charmed mesons decaying inclusively into electrons or positrons are D^\pm ($B^{D^\pm \rightarrow e^\pm} = 16.0\%$), D^0, \bar{D}^0 ($B^{D^0, \bar{D}^0 \rightarrow e^\pm} = 6.53\%$), and D_s^\pm ($B^{D_s^\pm \rightarrow e^\pm} = 8\%$) and that the possible charmed baryons decaying inclusively into electrons or positrons are Λ_c and $\bar{\Lambda}_c$ ($B^{\Lambda_c, \bar{\Lambda}_c \rightarrow e^\pm} = 4.5\%$). Thus, we get

$$x = 0.14. \quad (30)$$

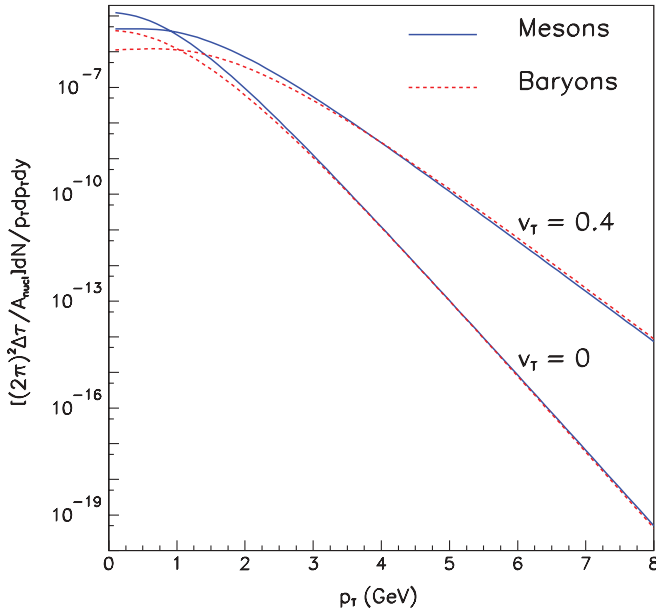


FIG. 3. (Color online) Charmed baryon and meson transverse-momentum distributions. The parameters used in the calculation are $m^B = 2.29$ GeV, $m^M = 1.87$ GeV, $\tau_0 = 1$ fm, $T_0 = 200$ MeV, and $T_f = 100$ MeV, corresponding to a final time $\tau_f = 8$ fm. Shown are the cases with $v_T = 0$ and $v_T = 0.4$.

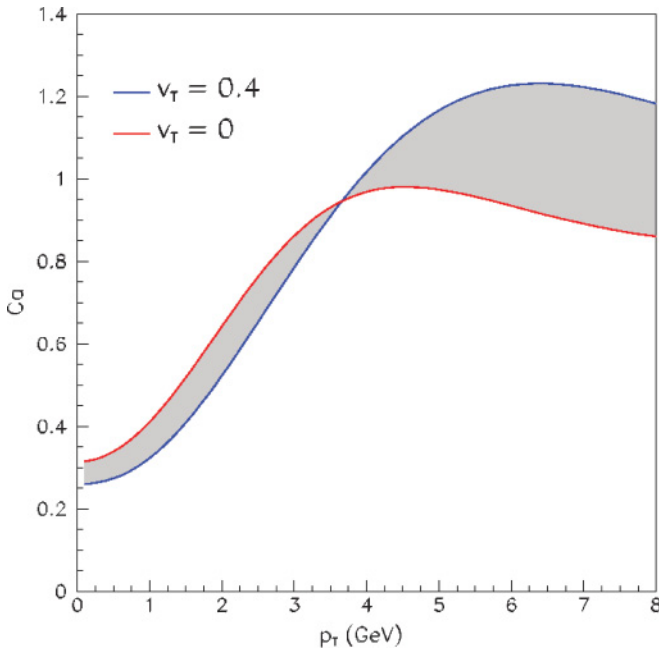


FIG. 4. (Color online) Charmed baryon-to-meson ratio, Ca , as a function of transverse momentum. The parameters used in the calculation are $m^B = 2.29$ GeV, $m^M = 1.87$ GeV, $\tau_0 = 1$ fm, $T_0 = 200$ MeV, and $T_f = 100$ MeV, corresponding to a final time $\tau_f = 8$ fm. Shown is a range when varying the transverse expansion velocity v_T from 0 (upper curve at low p_T) to 0.4 (lower curve at low p_T).

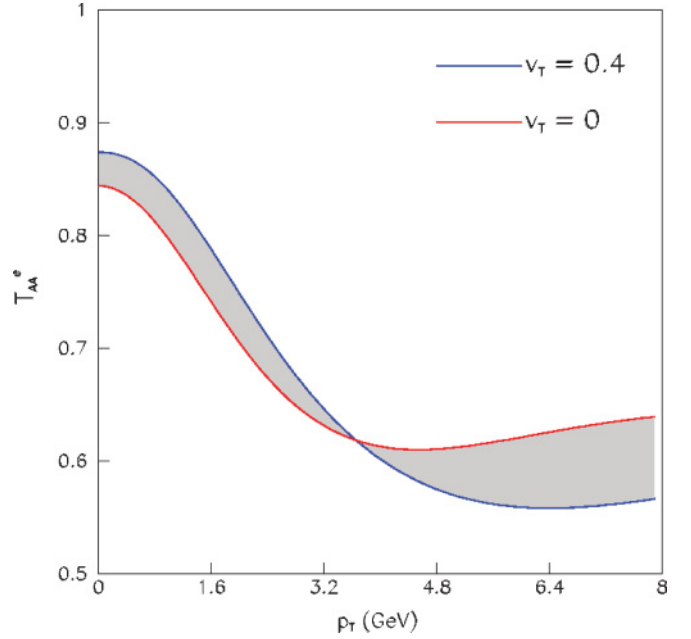


FIG. 5. (Color online) Suppression factor T_{AA}^e as a function of transverse momentum. The parameters used in the calculation are $m^B = 2.29$ GeV, $m^M = 1.87$ GeV, $\tau_0 = 1$ fm, $T_0 = 200$ MeV, and $T_f = 100$ MeV, corresponding to a final time $\tau_f = 8$ fm, $x = 0.14$, and $a = 0.073$. Shown is a range for the transverse expansion velocity from $v_T = 0$ (lower curve at low p_T) to $v_T = 0.4$ (upper curve at low p_T).

We also approximate the masses of all the charmed mesons considered to be equal to the mass of the D^\pm mesons.

From Eq. (6), we see that, without integrating over p_T , the dependence on the transverse momentum comes from $a = (dN_{pp}^\Lambda/dp_T)/(dN_{pp}^D/dp_T)$ and the product $Ca = (dN_{AA}^\Lambda/dp_T)/(dN_{AA}^D/dp_T)$. The integrated ratio a^{int} has been computed in Ref. [14] using a Pythia simulation, with the result $a^{\text{int}} = 0.073$. We have also performed a simulation using Pythia at next-to-leading order with 100,000 events and have found that with such statistics, the ratio of charmed baryons to charmed mesons in $p + p$ collisions at $\sqrt{s_{NN}} = 200$ GeV is flat up to $p_T \simeq 5$ GeV and consistent with the value reported in Ref. [14]. Therefore, for simplicity, we take a as a constant equal to the previously quoted number. Thus,

$$T_{AA}^e \simeq \frac{(1 + a^{\text{int}}) 1 + x(dN_{AA}^\Lambda/dp_T)(dN_{AA}^D/dp_T)}{(1 + xa^{\text{int}}) 1 + (dN_{AA}^\Lambda/dp_T)/(dN_{AA}^D/dp_T)}. \quad (31)$$

Figure 5 shows T_{AA}^e as a function of p_T . We have used a range of values for the transverse expansion velocity between $v_T = 0$ and $v_T = 0.4$. We see that for the chosen evolution parameters, T_{AA}^e is indeed smaller than 1, and thus, it contributes to the suppression of the single, nonphotonuclear modification factor R_{AA}^e .

VI. CONCLUSIONS

In this work we have shown that the anomalous suppression of the single, nonphotonuclear modification factor

R_{AA}^e can be partially understood by realizing that this quantity is affected by an enhancement in the charmed baryon-to-meson ratio at intermediate p_T in $Au + Au$ collisions. This enhancement happens because in this region, thermal recombination becomes the dominant mechanism for hadron production. We have made use of the DQRM to calculate this ratio and have shown that for moderate and even for vanishing transverse expansion velocities, it indeed can be larger than the charmed baryon-to-meson ratio in $p + p$ collisions. This enhancement in turn produces that the function T_{AA}^e is below 1 and thus contributes to the suppression factor introduced by considering energy losses caused by the propagation of heavy flavors in the plasma.

It is worth noting some important features concerning the results of this calculation: First, notice that we have not included the momentum shift introduced by energy losses when computing the transverse distributions of charmed mesons and baryons. This is so because for R_{AA}^e , energy losses should be included in the prefactor of the function T_{AA}^e . In this sense, to avoid a double counting of the effect, the ratio that goes into the calculation of this last function is the *raw* ratio. Second, it is expected that at some value of p_T , fragmentation becomes the dominant mechanism for hadron production and, therefore,

that the charmed baryon-to-meson ratio decreases above that p_T value, given that fragmentation produces more mesons than baryons. Third, we have considered finite values of transverse flow for charmed mesons and baryons even though it might be questionable that heavy flavors also flow as light flavors do. Nevertheless, there seems to be some experimental support for heavy-quark flow [29]. In this sense, the flow strength range we have considered is only for moderate values. Notice, however, that even in the absence of flow, the suppression factor keeps being less than 1. Some of these issues will be the subject of a future work to appear elsewhere.

ACKNOWLEDGMENTS

The authors are grateful to N. Armesto for very insightful comments and suggestions. A.A. wishes to thank the kind hospitality of both faculty and staff at CBPF during a sabbatical visit. Support for this work has been received in part by FAPERJ under Project No. E-26/110.166/2009, CNPq, the Brazilian Council for Science and Technology, DGAPA-UNAM under PAPIIT Grant No. IN116008, and CONACyT-México.

-
- [1] S. S. Adler *et al.* (PHENIX Collaboration), Phys. Rev. Lett. **96**, 032301 (2006).
 - [2] B. I. Abelev *et al.* (STAR Collaboration), Phys. Rev. Lett. **98**, 192301 (2007); A. G. Knospe (STAR Collaboration), Eur. Phys. J. C **62**, 223 (2009).
 - [3] M. Djordjevic *et al.*, Phys. Lett. **B632**, 81 (2006).
 - [4] N. Armesto *et al.*, Phys. Lett. **B637**, 362 (2006).
 - [5] S. Wicks *et al.*, Nucl. Phys. **A784**, 426 (2007).
 - [6] Y. L. Dokshitzer and D. E. Kharzeev, Phys. Lett. **B519**, 199 (2001).
 - [7] M. Djordjevic and M. Gyulassy, Nucl. Phys. **A733**, 265 (2004).
 - [8] B.-W. Zhang, E. Wang, and X.-N. Wang, Phys. Rev. Lett. **93**, 072301 (2004).
 - [9] N. Armesto, C. A. Salgado, and U. A. Wiedemann, Phys. Rev. D **69**, 114003 (2004).
 - [10] M. G. Mustafa, Phys. Rev. C **72**, 014905 (2005).
 - [11] M. Djordjevic, Phys. Rev. C **74**, 064907 (2006).
 - [12] M. Djordjevic and U. Heinz, Phys. Rev. C **77**, 024905 (2008); Phys. Rev. Lett. **101**, 022302 (2008).
 - [13] P. R. Sorensen and X. Dong, Phys. Rev. C **74**, 024902 (2006).
 - [14] G. Martinez-Garcia, S. Gadrat, and P. Crochet, arXiv:hep-ph/0702035; G. Martinez-Garcia, S. Gadrat, and P. Crochet, Phys. Lett. **B663**, 55 (2008); [Erratum-*ibid.* **B666**, 533 (2008)].
 - [15] S. S. Adler *et al.* (PHENIX Collaboration), Phys. Rev. C **69**, 034909 (2004).
 - [16] J. Adams *et al.* (STAR Collaboration), arXiv:nucl-ex/0601042.
 - [17] A. László and T. Schuster (NA49 Collaboration), Nucl. Phys. **A774**, 473 (2006).
 - [18] B. I. Abelev *et al.* (STAR Collaboration), Phys. Lett. **B655**, 104 (2007).
 - [19] Y. Oh and C. M. Ko, Phys. Rev. C **79**, 067902 (2009).
 - [20] R. C. Hwa and C. B. Yang, Phys. Rev. C **67**, 034902 (2003); V. Greco, C. M. Ko, and P. Lévai, Phys. Rev. Lett. **90**, 202302 (2003); R. J. Fries, B. Müller, C. Nonaka, and S. A. Bass, *ibid.* **90**, 202303 (2003).
 - [21] F. Karsch, E. Laermann, and A. Peikert, Phys. Lett. **B478**, 447 (2000); F. Karsch, Lect. Notes Phys. **583**, 209 (2002).
 - [22] A. Ayala, M. Martinez, G. Paić, and G. T. Sánchez, Phys. Rev. C **77**, 044901 (2008).
 - [23] W. Cassing and E. L. Bratkovskaya, Phys. Rev. C **78**, 034919 (2008); L. Ravagli, H. van Hees, and R. Rapp, *ibid.* **79**, 064902 (2009).
 - [24] H. van Hees and R. Rapp, Phys. Rev. C **71**, 034907 (2005); H. van Hees, V. Greco, and R. Rapp, *ibid.* **73**, 034913 (2006); H. van Hees, M. Mannarelli, V. Greco, and R. Rapp, Phys. Rev. Lett. **100**, 192301 (2008).
 - [25] G. D. Moore and D. Teaney, Phys. Rev. C **71**, 064904 (2005).
 - [26] C. J. Horowitz, E. J. Moniz, and J. W. Negele, Phys. Rev. D **31**, 1689 (1985).
 - [27] C. Horowitz and J. Piekarewicz, Nucl. Phys. **A536**, 669 (1992).
 - [28] G. T. Sánchez and J. Piekarewicz, Phys. Rev. C **65**, 045208 (2002).
 - [29] S. A. Butsyk (PHENIX Collaboration), Nucl. Phys. **A774**, 669 (2006).